COBEM 99
XV Congresso Brasileiro de Engenharia Mecânica
15th Brazilian Congress of Mechanical Engineering
22 - 26 de Novembro de 1999 / November 22 - 26, 1999 Águas de Lindóia, São Paulo,

NUMERICAL AND EXPERIMENTAL ANALYSIS OF THE NATURAL CONVECTION IN CAVITIES WITH PROTRUDING HEAT SOURCES AT THE BASE

Ricardo A. V. Ramos
DEM/FEIS/UNESP – Email: ramos@dem.feis.unesp.br
P.O. Box 31 – Zip Code 15385-000 – Ilha Solteira, SP, Brazil.
Gabriel C. Campos
ETSII/UPC – Email: ei35123740@est.etseib.upc.es
Zip Code 08032 – Barcelona, Spain.
Luiz F. Milanez
DE/FEM/UNICAMP – Email: milanez@fem.unicamp.br
P.O. Box 6122 – Zip Code 13083-970 – Campinas, SP, Brazil.

Abstract. *In this work a numerical and experimental analysis of the natural convection in a cavity with protruding heat sources mounted on the base and cooled laterally is performed. In the numerical solution the flow is assumed in steady state, laminar and two-dimensional. The fluid physical properties do not vary with temperature, thermal radiation is neglected and the Boussinesq approximation is adopted. The finite volume method is employed for the discretization of the equations and the numerical solution is obtained by using the SIMPLE algorithm. The velocity and temperature fields in the flow are obtained. In the experimental work, the temperatures are measured by means of thermocouples fixed in the upper and lower surfaces and also by means of a traversing probe that allows to take measurements in the flow field. The effect of the sources dissipation rates, the cavity aspect ratio and the lateral walls temperature on the sources temperature is observed. The temperature profiles in the cavity floor, as well the flow field temperatures are traced and a reasonable agreement between numerical and experimental results was found.*

Key words: *Natural convection, Electronic components, Thermal cavity.*

1. INTRODUCTION

The increasing technological development of the electronic industries permits the fabrication of very small components, resulting in a corresponding increase of the heat fluxes per unit volume and, consequently, of the temperature levels. This can cause an increase in the failure rate of the component, because the thermal deterioration factor varies almost exponentially with temperature. The energy dissipated must be effectively removed to keep

the temperature levels below the critical limit. Among the several existent mechanisms to remove the heat, natural convection is preferred, if possible, due to the simplicity and because it does not rely on other devices.

For a discussion on the thermal management and control of electronic equipment see, for example: Baum (1969), Scott (1974), Kraus & Bar-Cohen (1983), Incropera (1988), Nakayama & Bergles (1990), Peterson & Ortega (1990) and Bar-Cohen (1992), among others.

There is a number of more specific numerical and/or experimental works dealing with the components as protruding heat sources that partially block the flow: Kelleher *et al*. (1985); Afrid & Zebib (1987), Shakerin (1987), Nickell *et al.* (1987), Chen & Kuo (1988), Shakerin *et al*. (1988) and Ramos *et al.* (1998), among others.

In the present work a numerical and experimental analysis of the natural convection in a cavity with protruding heat sources, simulating electronic components, mounted on the cavity base, is conducted. The cavity is laterally cooled, as shown in Figure 1.

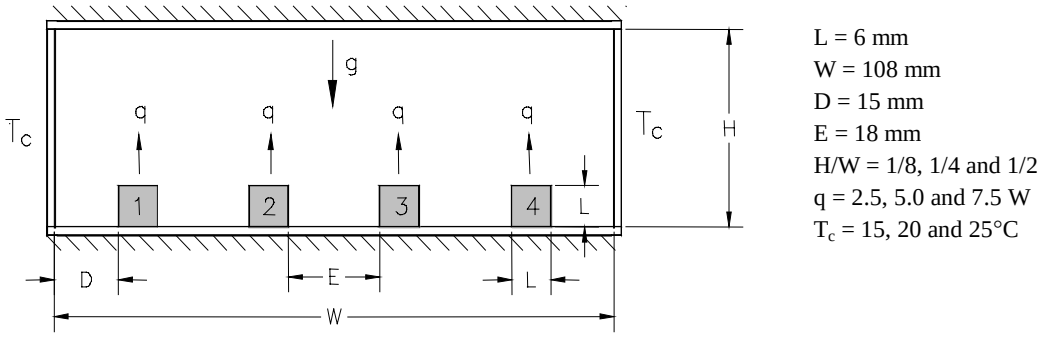

Figure 1: Cavity with protruding heat sources at the base.

2. NUMERICAL ANALYSIS

2.1 Assumptions

The flow is considered laminar, two-dimensional and in steady state. The physical properties do not vary with temperature, thermal radiation is neglected and the usual Boussinesq approximation is adopted.

2.2 Dimensionless Variables

The following dimensionless variables were used:

Distances: $x^* = x / L$ and $y^* = y / L$

Velocities: $u^* = u /(\alpha / L)$ and $v^* = v /(\alpha / L)$

Pressure: $P^* = P /[\rho(\alpha / L)^2]$

Temperature: $T^* = (T - T_\infty) / (qL^2 / k_f)$

Modified Rayleigh number: $Ra_q = g\beta qL^5 /(k_f \alpha \nu)$

Source term: $S^* = k_s / k_f$ (sources) or $S^* = 0$ (fluid)

Properties: $k^* = k_s / k_f$ and $\mu^* = \infty$ (sources) or $k^* = 1$ and $\mu^* = 1$ (fluid)

2.3 Formulation

The governing equations can be written in dimensionless form:

$$\frac{\partial u^*}{\partial x^*} + \frac{\partial v^*}{\partial y^*} = 0 \tag{1}$$

$$u^* \frac{\partial u^*}{\partial x^*} + v^* \frac{\partial u^*}{\partial y^*} = -\frac{\partial P^*}{\partial x^*} + \mu^* Pr \left(\frac{\partial^2 u^*}{\partial x^{*2}} + \frac{\partial^2 u^*}{\partial y^{*2}} \right) \tag{2}$$

$$u^* \frac{\partial v^*}{\partial x^*} + v^* \frac{\partial v^*}{\partial y^*} = -\frac{\partial P^*}{\partial y^*} + \mu^* Pr \left(\frac{\partial^2 v^*}{\partial x^{*2}} + \frac{\partial^2 v^*}{\partial y^{*2}} \right) + Ra_q PrT^* \tag{3}$$

$$u^* \frac{\partial T^*}{\partial x^*} + v^* \frac{\partial T^*}{\partial y^*} = k^* \left(\frac{\partial^2 T^*}{\partial x^{*2}} + \frac{\partial^2 T^*}{\partial y^{*2}} \right) + S^* \tag{4}$$

2.4 Average Nusselt Number

The average Nusselt number in the source faces can be determined through the coupling of the conduction-convection equations at the interface (i), resulting:

$$\overline{Nu}_i = -\frac{L}{P} \int_0^P \frac{1}{T_i^*} \left(\frac{\partial T^*}{\partial \eta^*} \right) d\varphi^* \tag{5}$$

where:

φ^* : generalized coordinate (direction x^* or y^*);

η^* : generalized coordinate (x^* for direction y or y^* for direction x);

P : perimeter of the source ($3L$);

i : refers to the interface.

2.5 Boundary Conditions

All the surfaces are impermeable and the no slip condition is assumed. Furthermore, the upper and lower surfaces are adiabatic. Therefore:

At the side walls ($x^* = 0$ and $x^* = W/L$): $u^* = v^* = T^* = 0$ (6)

At the base ($y^* = 0$) and at the top ($y^* = H/L$): $u^* = v^* = \dfrac{\partial T^*}{\partial y^*} = 0$ (7)

2.6 Grid

Structured non-uniform grids were used with smaller and constant spacing along the sources where the gradients are more pronounced, with a smooth increase in the spacing from this region. Grids were generated according to a distribution function based in the power law, at a rate less 10%, because sudden changes in the spacing can introduce numerical instabilities, as explained by Roache (1976).

2.7 Method

The numerical solution of this problem was obtained by using the Finite Volume Method with the Power Law scheme and the SIMPLE (Semi-Implicit Method for Pressure-Linked Equations) algorithm due to Patankar (1980).

2.8 Convergence Criterion

The convergence criterion of the iterative process was as follows:

$$\xi = \max \left| \frac{\phi_{i,j}^{(n)} - \phi_{i,j}^{(n-1)}}{\phi_{i,j}^{(n)}} \right| \leq 10^{-4} \quad (8)$$

where:

ξ : admitted tolerance;

ϕ : generalized parameter (u^*, v^* or T^*);

n : referent to the n-th iteration;

i,j : position of the point in the domain.

3. EXPERIMENTAL ANALYSIS

A cavity was built with aluminum lateral surfaces, maintained at a constant temperature by means of a thermostatic bath. The upper and lower surfaces are made of epoxy and are thermally insulated from the external ambient by Styrofoam. The sources are constituted of a set of resistors in parallel, electrically insulated and covered by a 165 mm long aluminum bar of 6×6 mm section, to simulate the shape of an electronic component. Thermal paste was used in the assembly of the sources on the board to reduce thermal contact resistance. All temperature measurements were made by type J thermocouples (Iron-Constantan) AWG-32, using a digital multimeter of 4½ digits, coupled to a computer and to a compensation system (cold junction). The measuring locations are indicated in Figure 2.

Figure 3 shows part of the experimental apparatus. The complete experimental assembly and more details about the procedure can be found in Ramos *et al.* (1998).

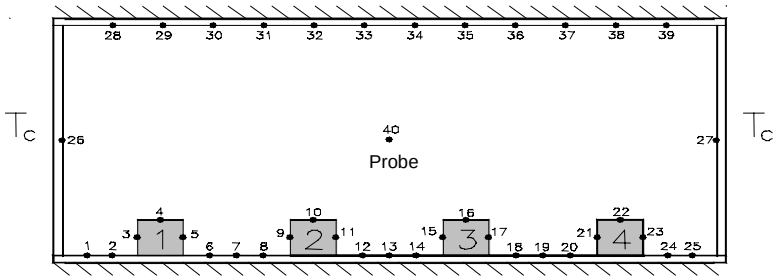

Figure 2: Position of the thermocouples in the cavity.

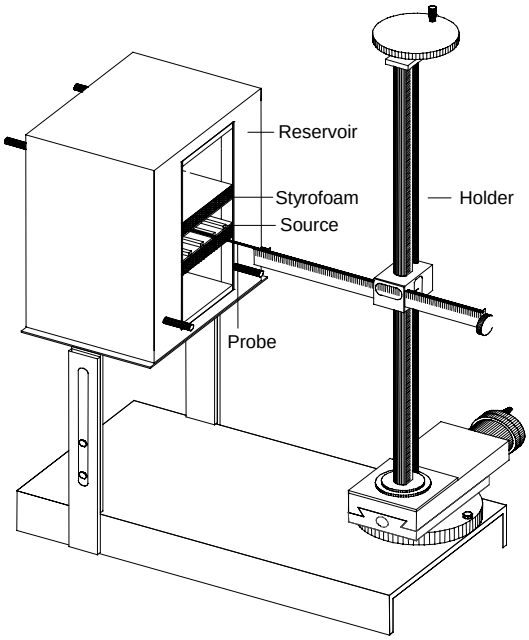

Figure 3: Part of the experimental apparatus.

4. PROCEDURE

In order to observe the influence of the cavity aspect ratio on the sources temperature, three values were considered, H/W = 0.125, 0.25 and 0.5.The effect of the temperature of the lateral walls were also verified considering T_c = 15, 20 and 25°C. The power dissipated in each source was 2.5, 5.0 and 7.5 W, corresponding to Ra_q = 0.8×10^4, 1.6×10^4 and 2.4×10^4, respectively, with the physical properties considered at 60°C. Thus, the ratio of the thermal conductivities of the source (aluminum) and of the air is expressed by k_s / k_f = 7285 (Bejan, 1996). In this case, the size of the source was used as the characteristic length (L = 6 mm).

A parametric analysis was conducted based on the configuration: H/W = 0.25, T_c = 20°C and Ra_q = 1.6×10^4; two of these values were always used and the other was varied within the range considered, in order to study the influence of each parameter on the flow, resulting in the cases presented in Table 1, where the bold number represent the values that vary respective to the baseline case considered (case 2). The maximum flow temperature was taken as the control parameter because it is directly related to the heat transfer in the flow.

Table 1: Description of the cases to be considered.

Cases	Ra_q	H/W	T_c [°C]
(1)	**0.8×10^4**	0.25	20
(2)	1.6×10^4	0.25	20
(3)	**2.4×10^4**	0.25	20
(4)	1.6×10^4	**0.125**	20
(5)	1.6×10^4	**0.5**	20
(6)	1.6×10^4	0.25	**15**
(7)	1.6×10^4	0.25	**25**

5. RESULTS

Grid tests were initially made for each of the cases to be studied numerically, utilizing the values of the basic configuration, with the maximum flow temperature taken as the control parameter. Figure 4 is only a form representation of the grids tested. The grids selected are presented in Table 2.

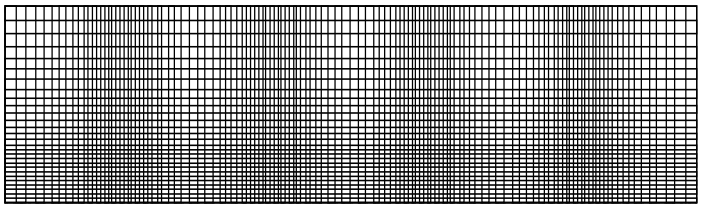

Figure 4: Form of the grid used in the numerical solution.

Table 2: Grids used in the numerical solution.

Aspect ratio	Number of grid points	Number of volumes on the sources	Total number of volumes
0.125	262×42	400	10400
0.25	262×62	400	15600
0.50	262×102	400	26000

The average Nusselt number of the sources (Nu_i), as well as the maximum temperature in the cavity floor (Tp_{max}), obtained numerically are shown in Table 3.

Figures 5 to 7 show the numerical results of the effect of the power dissipated in the sources, of the cavity aspect ratio and of the cooling temperature of the lateral walls, on the temperature of the cavity floor (Tp), where the sources are mounted.

Table 3: Average Nusselt number in the sources and maximum temperature.

Cases	$\overline{Nu_1} = \overline{Nu_4}$	$\overline{Nu_2} = \overline{Nu_3}$	Tp_{max} [°C]
(1)	6.21	1.94	110.3
(2)	6.82	2.17	134.0
(3)	7.24	2.36	176.9
(4)	5.41	0.38	212.5
(5)	8.97	2.88	124.3
(6)	6.82	2.17	129.0
(7)	6.82	2.17	139.0

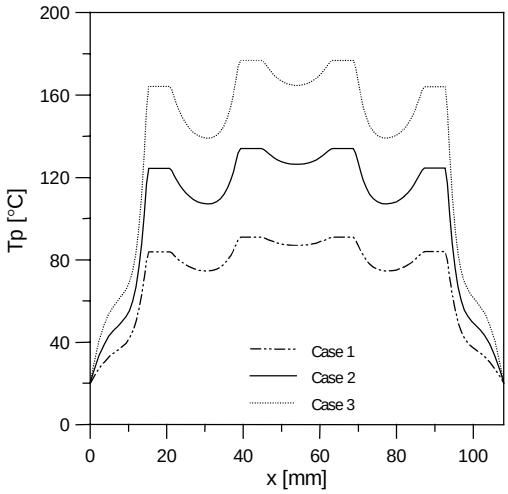

Figure 5: *Tp* in the cavity as a function of the power dissipated.

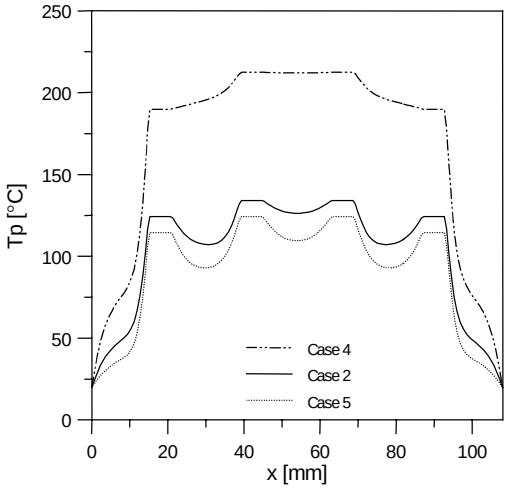

Figure 6: *Tp* in the cavity as a function of the aspect ratio.

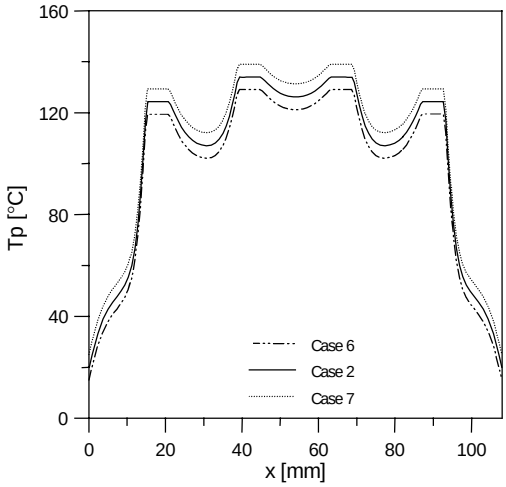

Figure 7: *Tp* in the cavity as a function of the side walls temperature.

Streamlines and isotherms obtained numerically are shown in Figures 8 and 9, respectively. Figure 10 shows the isotherms obtained by the interpolation of the experimental data measured in twenty five positions in five sections of the flow (y = 0, H/4, H/2, 3/4H and H), for the basic configuration considered (case 2).

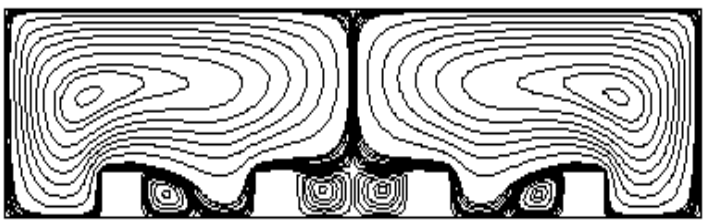

Figure 8: Streamlines obtained numerically (case 2).

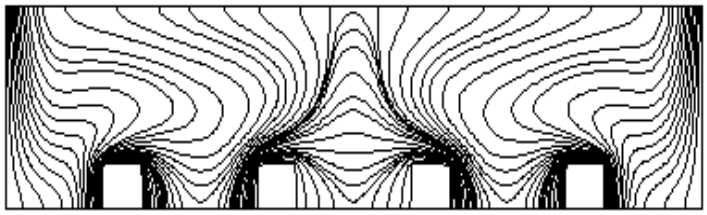

Figure 9: Isotherms obtained numerically (case 2).

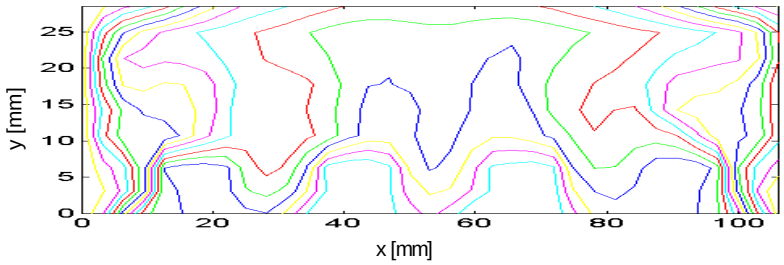

Figure 10: Isotherms obtained experimentally (case 2).

The temperature profiles in several flow sections (y = 0, 1/4H, 1/2H, 3/4H and H), obtained experimentally through the traversing probe and by thermocouples installed in the upper and lower surfaces of the cavity were presented previously by Ramos *et al.* (1998), for each one of the cases studied. Figure 11 shows a comparison of the temperature profiles of the lower surface of the thermal cavity obtained numerically and experimentally for the baseline case considered.

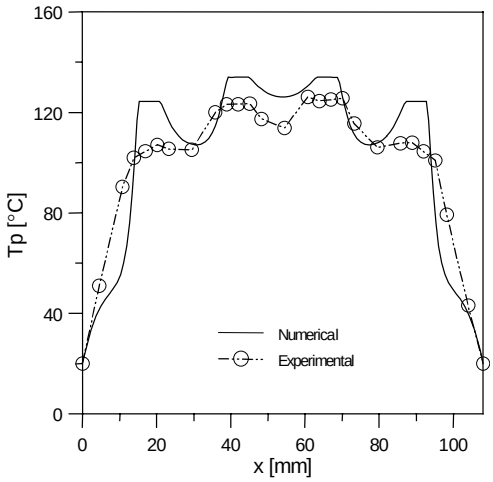

Figure 11: Numerical and experimental temperature distribution in the cavity floor (case 2).

6. CONCLUSIONS

The streamlines illustrate the air movement inside the cavity and how the protruding sources block the flow, affecting the lines in this region. Also, the formation of recirculation cells can be observed between the sources. Although not shown in this work, the formation of more recirculation cells was observed as the power dissipated increases, or the cavity aspect

ratio decreases. The isotherms represent the temperature gradient that the flow is subjected, and it may be noticed that, even though the sources dissipate the same amount of heat, the extreme sources (1 and 4) are more strongly influenced by the cooling of the lateral walls, exhibiting lower temperature levels than the inner sources (2 and 3).

By analyzing the temperature distribution in the lower surface, where the sources are mounted, we can conclude that as the power is increased, the temperature levels increase, and the same happens when the aspect ratio is decreased. It is also verified that the cooling temperature of the side walls practically does not influence the sources temperatures, because the range of variation is restricted and the differences between the temperatures of the sources and of the side walls is high.

Respective to the average Nusselt number in the sources, it may be noticed that the values for the sources in the extremes are always higher than that for the inner sources. When the power dissipated is increased, the values of the average Nusselt number increase moderately. When the aspect ratio is increased, a considerable increase in the values of the average Nusselt number is observed. The cooling temperature of the lateral wall does not interfere with the values of the average Nusselt number.

A reasonable similarity between the isotherms obtained numerically and experimentally was noticed for the baseline case considered. A better agreement could have been obtained with more experimental measurements, without the need to interpolate the data, thus permitting a better definition of the curves.

Comparing the numerical and experimental temperature profiles for the baseline case considered, it can be verified that they exhibit a reasonable agreement, and the differences can be attributed to the hypotheses used to simplify the numerical solution, such as to neglect the heat conduction at the base and the radiation and not to mention errors inherent to the experimental procedure.

Eventually, the multigrid technique will be implemented numerically, the variation of the physical properties with the temperature will be considered and experiments will be made for the determination of the flow velocity field, utilizing laser anemometer and/or flow visualization techniques.

7. REFERENCES

Afrid, M. & Zebib, A., 1987, Natural Convection Air Cooling of Heated Components Mounted on a Vertical Wall, in Temperature Fluid Measurement in Electronic Equipment, ASME HTD-Vol. 89, pp. 17-24.

Bar-Cohen, A., 1992, State of the Art in Thermal Packaging of Electronic Equipment, Journal of Electronic Packaging, Vol. 114, pp.257-270.

Baum, R., 1969, Handbook of Electronic Packaging, ed. by C. A. Harper, McGraw-Hill, Chapter 11: Thermal-Design Considerations for Packaging Electronic Equipment, p.1-56.

Bejan, A., 1996, Transferência de Calor, Ed. Edgard Blucher Ltda., 540p.

Bergles, A. E., 1991, The Evolution of Cooling Technology for Electrical, Electronic, and Microelectronics Equipment, Proceedings of 3rd ASME/JSME Thermal Engineering Joint Conference, Vol. 34, pp.1679-1693.

Chen, Y. M. & Kuo, Y., 1988, Studies on Natural Convection Heat Transfer from Arrays of Block-Like Heat-Generating Modules on a Vertical Plate, Proceedings of the 20th International Symposium on Heat Transfer in Electronic Equipment, Yugoslavia, pp.1-8.

Incropera, F. P., 1988, Convection Heat Transfer in Electronic Equipment Cooling, Journal of Heat Transfer, Vol. 110, pp.1097-1111.

Kelleher, M. D., Knock, R. H. & Yang, K. T., 1985, Laminar Natural Convection in a Rectangular Enclosure Due to a Heated Protrusion on One Vertical Wall - Part I: Experimental Investigation, Proceedings of the 23rd National Heat Transfer Conference, Heat Transfer in Electronic Equipment, Denver, pp.169-177.

Kraus, A. D. & Bar-Cohen, A., 1983, Thermal Analysis and Control of Electronic Equipment, McGraw-Hill, New York.

Nakayama, W. & Bergles, A. E., 1990, Cooling Electronic Equipment: Past, Present and Future, in Heat Transfer in Electronic and Microelectronics Equipment, pp.3-39.

Nickell, T. W., Ulrich, R. D. & Webb, B. W., 1987, Combined Natural Convection and Radiation Heat Transfer from Parallel Plates with Discrete Heat Sources, ASME Winter Annual Meeting, Boston, pp. 1-8.

Patankar, S. V., 1980, Numerical Heat Transfer and Fluid Flow, Washington, Hemisphere Publishing Corp., 197p.

Peterson, G. P. & Ortega, A., 1990, Thermal Control of Electronic Equipment and Devices, in Advances in Heat Transfer, Vol. 20, pp.181-314.

Ramos, R. A. V., Campos, G. C. & Milanez, L. F., 1998, Análise Experimental da Convecção Natural em uma Cavidade com Fontes de Calor Protuberantes na Superfície Inferior, Proceedings of the VII Brazilian Congress of Engineering and Thermal Science, Rio de Janeiro, RJ, pp.252-256.

Roache, P. J., 1976, Computational Fluid Mechanics, Hermosa Pub., New Mexico.

Scott, A. W., 1974, Cooling of Electronic Equipment, John Wiley & Sons, New York.

Shakerin, S., Bohn, M. & Loehrke, R. I., 1988, Natural Convection in an Enclosure with Discrete Roughness Elements on a Vertical Heated Wall, International Journal of Heat and Mass Transfer, Vol. 31, No. 7, pp.1423-1430.

Shakerin, S., 1987, Laminar Natural Convection on a Vertical Surface with Adiabatic Discrete Roughness, ASME HTD-Convective Transport, Vol. 82, pp.79-83.